NUMERICAL ANALYSIS OF A LARGE-SCALE LINEAR FRESNEL CSP PLANT AT STEADY-STATE CONDITION

S. Navid Ghavami Masooleh[1], Dominik Schlipf[1], Max Weidmann[1], Uwe Schnell[1], Hartmut Maier[2], Marcus Dohn[2] and Martin Stenglein[2]

[1] Universität Stuttgart, Institut für Feuerungs- und Kraftwerkstechnik (IFK), 70569 Stuttgart, Germany

[2] enolcon gmbh, 74321 Bietigheim-Bissingen, Germany

d_{in}	tube inner diameter, m	x	steam fraction, kg/kg
f_G	gas friction factor, -	Δh_i	specific enthalpy variation in segment i, kJ/kg
f_L	liquid friction factor, -	Δp_i	pressure variation in segment i, Pa
Fr_H	homogeneous Froude number, -	Δp_L	liquid pressure drop, Pa
h	specific enthalpy, kJ/kg	θ	angle of tube inclination,-
i	number of segment, -	μ_L	liquid dynamic viscosity, kg/ms
L	length, m	ρ_G	gas density, kg/m^3
$\dot{m}_{total}$	mass flux, kg/m^{2}s	ρ_H	homogeneous two-phase density, kg/m^3
p	pressure, Pa	ρ_L	liquid density, kg/m^3
$\dot{q}_i$	heat flow rate from wall to fluid, W/m^2	σ	liquid surface tension, N/m
T	temperature, °C	$\emptyset_{fr}^2$	two-phase friction multiplier,-
We_L	liquid Weber number, -		

1. Introduction

Thinking of the current emission reduction policies in the field of energy production, one of the key parameters is to increase the ratio of total efficiency over costs of the so-called “green” technologies. Solar power is currently one of the most attended eco-friendly technologies based on conversion of sunlight into electricity, either directly by photovoltaics (PV), or indirectly using concentrated solar power (CSP). Linear Fresnel CSP is one of the latter types, offering cost-effective energy production on large scales as an alternative to conventional power plants. It derives its name from an optical system, which uses thin, flat reflector panels to focus the sunlight on a fixed absorber tube located at a common focal point. The concentrated solar thermal energy is used to expand the water flow inside the absorber tubes and to produce pressurized hot steam in order to operate a heat engine (usually a steam turbine) connected to an electrical power generator. The heat may also be used to increase the temperature of some thermal oil flowing inside the absorber tubes; the oil then goes through a heat exchanger to boil water into steam.

The advantages of Linear Fresnel collectors include the relatively simple construction, low wind loads and significantly lower costs than similar technologies like parabolic trough collectors. However, a major challenge that must be addressed is the fluctuating intensity of the radiation changes during the day, which causes a substantial need for advanced control methods. Currently, control concepts are only available for small power plants (1-5 MW_{el}) of this type; so, a control engineering approach to build a solar thermal CSP with capacities more than 50 MW_{el} based on Linear Fresnel technology is missing. This deficiency inhibits further industrial application of this technology and leads to risk-related delays of investment decisions.

The presented work is part of an ongoing joint research project sponsored by the German Federal Ministry of Economics and Technology (BMWi) within the ZIM program (Central Innovation Program for small and medium sized businesses). The main goal of the project is to develop new technical security operations and systematic control methods to eliminate technical risks in large CSP plants based on Linear Fresnel technology. The main technical challenge is to investigate necessary components and control equipment hardware and software via model-based simulation to achieve continuous stable operation at full- and partial-load scenarios and under management of possible interferences with the optimum efficiency.

In this paper, different parameters of a solar evaporation field based on Linear Fresnel technology are described and general characteristics of the water-steam flow inside the multiple parallel absorber tubes of the field are introduced in detail. Thermal losses due to radiation and conduction and the overall efficiency are evaluated. Moreover, partial disturbances on the evaporation field, their sources, and their consequences are estimated. Then, the convection and evaporation processes inside the absorber tubes are simulated using computational fluid dynamics (CFD). The system behavior is also investigated at partial-load scenarios due to estimated disturbances. Afterwards, simulation results at different load scenarios are presented and different characteristics of the system are analyzed. Only the steady and quasi-steady working states are demonstrated, and transient conditions are not addressed here. Nevertheless, having a detailed overview on steady-states clarifies the path to modeling the dynamic behavior of the system, and therefore, provides further hints for the behavior of the system via transition from one state to another, as well as different control concepts for large-scale Linear Fresnel CSP plants.

2. Description of the overall setup

The concept of the solar steam generator is derived from the forced circulation steam boilers as in the conventional power plant technologies. The differences to the conventional boiler however arise e.g. from higher pressure losses, altering pressure loss in partial-load operation, quickly changing heat input, local separation of evaporator and superheater, a large boiler size, and ask for new technical solutions concerning the cycle arrangement and the operation. The design of the solar steam generator based on Linear Fresnel reflectors varies slightly depending on the technology supplier. These design variations may represent themselves in the form of e.g. wider and/or longer but still similar shaped mirrors, different receiver designs, size of base collector modules, etc. In this research, the Linear Fresnel system of the German company Novatec Solar GmbH (formerly known as Novatec Biosol AG) was chosen and is used as the basis. The model of a 50 MW_{el} power plant, using real power plant equipment data, has been set up in EBSILON® Professional to examine the influences of the solar boiler on the power plant operation in characteristic steady states. Figure 1 shows a simplified process flow diagram of a concentrated solar power plant producing saturated steam by means of a solar evaporation field.

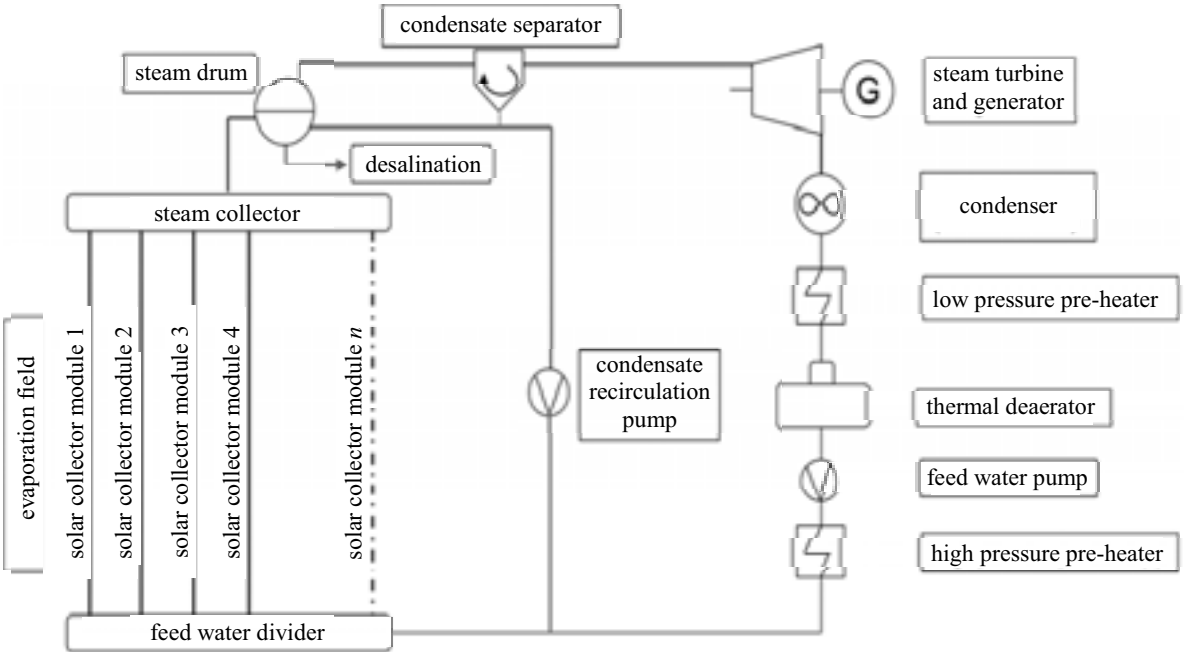

Figure 1: Simplified process flow diagram of the water-steam cycle in a Linear Fresnel CSP operating with saturated steam

In regards to conventional power plant equipment, none of the components which are shown and also those which are not shown here (e.g. a turbine bypass) is special customized equipment for CSP plants. The design of the equipment for a varying and foreseeable load change, as well as the daily start-up and shut-down of

the power plant (if no long-term thermal storage is applied), do not pose any difficult challenge. This has also been successfully proven in several CSP plants with different solar boiler technologies. Therefore, the only different part in comparison with conventional power plants is represented by the solar field that acts as a common steam boiler with a varying, but foreseeable fuel supply; the sun.

The main part of the collector field comprises multiple rows of reflectors, each consisting of several slightly curved mirrors attached to a support structure. Figure 2 shows the schematic layout of a Linear Fresnel collector module. All reflector panels in each row are connected together through a shaft (not shown here). This shaft is supported by bearings between each reflector and is connected to an actuator system for the adjustment of the reflectors and thus their focus in accordance with the sun position over the day.

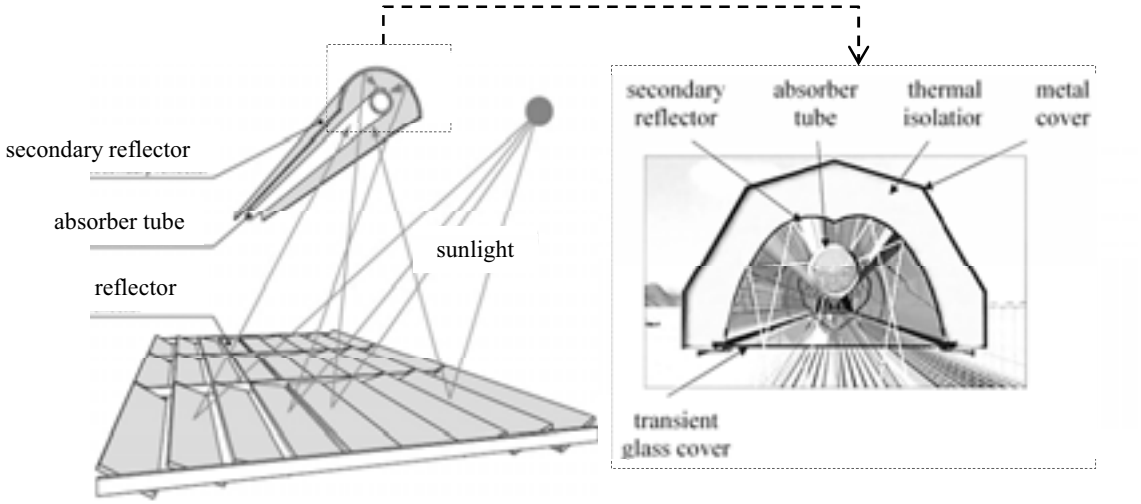

Figure 2: Principle of a Linear Fresnel basic solar collector module

In the case of the Novatec system, one basic solar collector module has a total length of 44.8 meters and a width of 16 m, approximately. These base modules are connected to each other along the length and arranged in parallel rows. Here, the reflector panels focus the sunlight onto the absorber tube, manufactured of stainless steel, with an outer diameter of approximately 70 millimeters. The absorber tube provides an attenuation coefficient of nearly 95% and an emissivity factor of maximum 10%. The amount of the reflected direct normal irradiation (DNI) depends on the reflectivity of the reflector panels and the transmittance of the glass cover below the tube, as well as other optical factors like cleanliness of the components. The absorber tube is installed inside a receiver system, uppermost covered by a thin layer of aluminum as the secondary reflector with an approximate reflection ability of 95%, which reflects stray irradiation on the tube.

Since the Linear Fresnel system operates with direct evaporation, water is preheated by heat exchangers before it is fed directly into the absorber tube at the inlet of the collector. During the preheating process, the water temperature rises up to a value below the saturation point. It is then directed via divider tubes to the parallel absorber tubes. In case of no disturbances in the entire field the total mass flow is equally distributed between all absorber tubes. In order to equalize the pressure at the inlet of the evaporation field, a hydraulic balancing must be done by choosing different tube diameters or by using orifice plates, regardless of the distance between the divider and the respective absorber tube. While flowing through the absorber tubes, the water is then fully heated up to the saturation point and evaporates. Accordingly, the generated fluid exits at the end of the evaporation field usually in the form of partially saturated steam and water at saturation temperature. The amount of heat contained by this mixture is considered as the measure of thermal energy, which is determined by the saturation temperature, mass and average specific heat of the fluid. Separation of the steam and water takes place inside a steam drum behind the evaporation field. This ensures that only saturated steam is sent towards the steam turbine. Finally, the steam is directed to the steam turbine where the thermal energy is converted into mechanical energy. In the case of a Linear Fresnel plant operating with superheated steam, the saturated steam is sent into the superheater solar field before the steam turbine.

3. CFD modeling of steady-state operational conditions

Solar thermal power plants use heat exchangers that are designed for consistent working conditions. However, the performance of the solar power plant, and particularly the solar evaporation field, endures physical circumstances such as DNI disparity during the day, change of seasonal heat capacity, partial or full cloud coverage, partial-load due to maintenance concerns, etc. Therefore, the performance must be studied under different geometrical, thermal, and mechanical boundary conditions in order to provide a clear interpretation of the sensitivity of the model. This defines the need of knowledge about the extent and sources of different load disturbances, as well as detailed consequences of different working conditions on the performance of the plant.

The one-dimensional CFD program "WaDa" (Weidmann 2009), designed by the "Institut für Feuerungs- und Kraftwerkstechnik", University of Stuttgart, and adapted for the simulation of the water-steam cycle in CSP plants, calculates a steady-state solution for a heated tube system. All tubes are discretized by a finite number of volumetric segments. The state of fluid is clearly defined by pressure and enthalpy in each segment. To achieve a state of equilibrium, the given initial conditions have to be adapted iteratively to the governing fluid dynamic conditions. Therefore, a momentum balance is drawn in each segment depending on velocity, the inclination and density, resulting in a pressure difference over the segment length. Since the pressure at the end of a tube system is usually given, e.g. by a turbine, it is set as a boundary condition. The current pressure at the beginning of the tube system is calculated contrary to the flow direction by deduction of each segment's pressure difference from the previous one. This begins at the end of the tube system (segment n):

$$p_i = p_{n+1} - \sum_{i=k}^{n} \Delta p_i \qquad k = n, \dots, 1 \tag{Eq. 1}$$

The pressure drop of one- and two-phase flows through evaporator tubes and connecting pipes is composed of the three components frictional, static and acceleration pressure drop.

$$\Delta p_i = (\Delta p_i)_{friction} + (\Delta p_i)_{static} + (\Delta p_i)_{acceleration} \tag{Eq. 2}$$

Special attention has to be drawn to the two phase flow in the evaporator, since the conditions are not supercritical. The existence of two phases over a long distance in the evaporator causes additional pressure losses due to momentum interaction. This phenomenon is considered by the introduction of the Friedel (Friedel 1978) two phase method, which utilizes a two phase multiplier:

$$\Delta p_{frict} = \Delta p_L \emptyset_{fr}^2 \tag{Eq. 3}$$

where Δp_L is calculated for the liquid-phase flow as:

$$\Delta p_L = f_L (L/d_{in}) \dot{m}_{total}^2 (1/(2\rho_L)) \tag{Eq. 4}$$

The liquid friction factor is obtained by eq. 5, assuming there is only water flowing inside the tube:

$$f_L = \frac{0.3164}{\left(\frac{\dot{m}_{total} d_{in}}{\mu_L}\right)^{1/4}} \tag{Eq. 5}$$

The two-phase multiplier is defined as:

$$\emptyset_{fr}^2 = E + \frac{3.24FH}{Fr_H^{0.045} We_L^{0.035}} \tag{Eq. 6}$$

where the dimensionless factors E, F, H, Fr_H, We_L are as follows:

$$Fr_H = \frac{\dot{m}_{total}^2}{g d_{in} \rho_H^2} \quad \text{(Eq. 7)}$$

$$E = (1-x)^2 + x^2 \frac{\rho_L f_G}{\rho_G f_L} \quad \text{(Eq. 8)}$$

$$F = x^{0.78}(1-x)^{0.224} \quad \text{(Eq. 9)}$$

$$H = \left(\frac{\rho_L}{\rho_G}\right)^{0.91} \left(\frac{\mu_G}{\mu_L}\right)^{0.19} \left(1 - \frac{\mu_G}{\mu_L}\right)^{0.7} \quad \text{(Eq. 10)}$$

$$We_L = \frac{\dot{m}_{total}^2 d_{in}}{\sigma \rho_H} \quad \text{(Eq. 11)}$$

The homogeneous density is calculated based on the steam content of the flow:

$$\rho_H = \left(\frac{x}{\rho_G} + \frac{1-x}{\rho_L}\right)^{-1} \quad \text{(Eq. 12)}$$

For calculation of the enthalpy, the process is in reverse sequence compared to the pressure calculation (relating to the flow direction). Since pressure and temperature are now known at the beginning of the tube system, the enthalpy is determined by:

$$h_1 = h(p_1, T_1) \quad \text{(Eq. 13)}$$

and set as a boundary condition in the first segment. An energy balance is calculated for each segment resulting in an enthalpy difference which depends on the supplied heat, the pressure difference and the dissipative heat from friction losses. Now the first segment's enthalpy is taken as an initial condition to which the enthalpy differences of all segments are added. So a new steady state is achieved. Figure 3 shows the finite volume discretization scheme for the calculation of fluid characteristics in all segments of the tube.

$$h_{i+1} = h_1 + \sum_{i=0}^{k} \Delta h_i \qquad k = 1, \dots, n \quad \text{(Eq. 14)}$$

$$\Delta h_i = \frac{\dot{q}_i}{\dot{m} A_i} + \frac{1}{\rho_i} \Delta p_i \quad \text{(Eq. 15)}$$

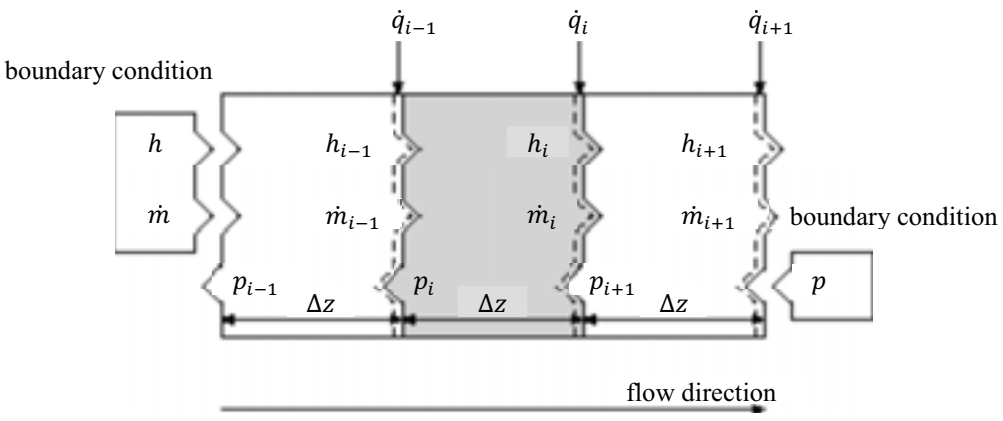

Figure 3: Axial discretization of a tube into multiple volumetric segments

In the following chapter, the performance of the evaporation field is examined by studying different boundary and load conditions using CFD simulations. All simulations are done for stationary working conditions. Accordingly, the mixture of water-steam remains under thermodynamic equilibrium at all working states.

4. Simulation results

Several simulations were done for the evaporation field of the plant described in chapter 2. The overall setup is summarized in table 1. The first layout consists of 47 absorber tubes that are divided in five different modules. Four of the modules include ten absorber tubes and the last module contains the remaining seven. The length of one absorber tube is set to 806.4 meters (18 base collectors in a row). The second layout consists of 94 absorber tubes divided into fourteen different modules whereas each contains 7 absorber tubes except for the last module. In this layout the length of each absorber tube is set to 403.2 meters (9 base collectors in a row). Both layouts engross the same extent of land. For every module a detached water-steam collector and feed water distributor are used. Each module is connected to the steam drum by an individual tube. The same structure is used for the connection between the feed water storage and the distributors.

Table 1: Geometrical dimensions of the simulated solar evaporation field

	Each absorber tube			**Entire evaporation field**	
	Length	Inner diameter	# base modules	Total width	# absorber tubes
Layout 1	806.4 m	0.062 m	18	960 m	47
Layout 2	403.2 m	0.062 m	9	1920 m	94

As boundary conditions, the temperature in the absorber tubes inlet is set to 175 °C. The pressure at the steam drum is set to 70 bar, which results in a saturation temperature of 285 °C. In this case a steam content of approximately 80% is expected.

The following simulations were done for both layouts, but only the results for layout 1 are shown if there is no big difference observed between the layouts. First of all, the behavior of a single absorber tube is shown, and then the behavior of the entire field is analyzed.

4.1 *Behavior of a single absorber tube at different geometrical conditions*

In this first simulation the behavior of a single absorber tube is analyzed. A big effort was made to calculate the pressure drop of the flow inside the tubes. Figure 4 (left) shows the pressure variation along an absorber tube. As previously described, the pressure is calculated against the general flow direction, since it is assumed that the outlet pressure is defined by the steam turbine. In the single-phase flow area (approximately up to 250 meters), the pressure is linearly decreasing. However, once the evaporation starts the influence of the two-phase pressure drop results in a nearly parabolic decrease of pressure. The amplitude of Δp_i increases at higher steam contents leading to more than 90% of the total pressure drop occurring in the two-phase flow area.

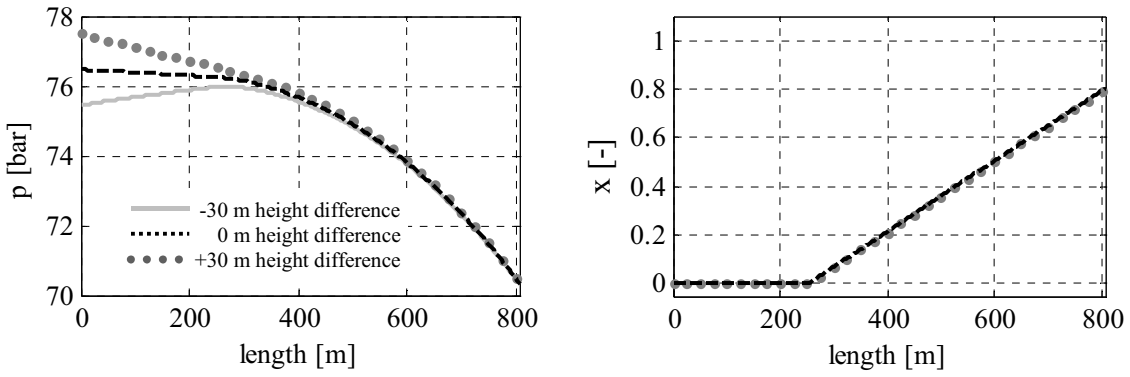

Figure 4: Variation of pressure (left) and steam content (right) along a single absorber tube

In general, the evaporation field is modeled on a fully horizontal surface. In order to have a better understanding of the influence of this geometrical boundary condition on the pressure drop, the behavior of the system is investigated applying ±30 meters height difference between the two heads of all absorber tubes. Figure 4 shows the pressure variation along an absorber tube. The influence of the height difference is significant only in the single-phase flow area (up to 250 meters in layout 1), while it can be neglected during the two-phase flow. This can be explained from two different points of view. (1) The amount of the friction pressure drop significantly increases in the two-phase flow area and dominates the two other components at higher steam contents. (2) Besides, according to eq. 16, the amount of static pressure drop is a linear function of the fluid density, decreasing as the steam content increases in the two-phase flow area:

$$(\Delta p_i)_{static} = \rho_i g \Delta L_i \sin\theta \qquad \text{(Eq. 16)}$$

Figure 5 shows the quick reduction of the fluid density at onset of the evaporation process, and consequently, the two-phase flow. Figure 4 shows that the proceeding evaporation process leads to elimination of the static pressure drop compared to the friction component and makes the total pressure independent of the inclinations.

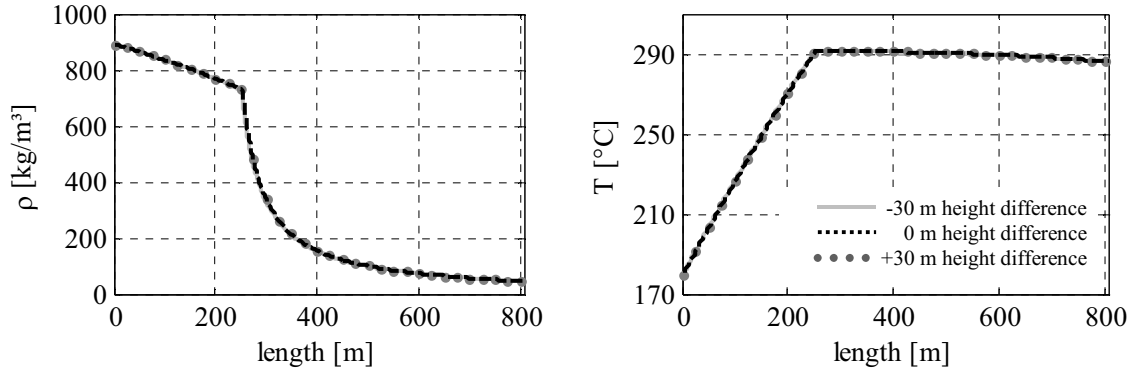

Figure 5: Variation of density (left) and temperature (right) along a single absorber tube

As previously shown in figure 1, several absorber tubes are connected to a steam collector and a feed water distributor, respectively at the outlet and the inlet of the evaporation field. Every distributor has its own divider tube connecting the relevant solar collector module to the feed water storage. Due to the long width of the evaporation field, the distance of the feed water storage and the solar collector modules at the edges of the evaporation field is much larger than of those in the center of the field. For layout 1 the length of the longest divider tube is about 400 meters, while for layout 2 this length increases up to more than 850 meters. This provides the necessity of considering additional pressure drop caused by the extreme length of the divider tubes. Figure 6 shows the pressure variation through the entire divider, absorber and collector tubes relevant to the furthermost module.

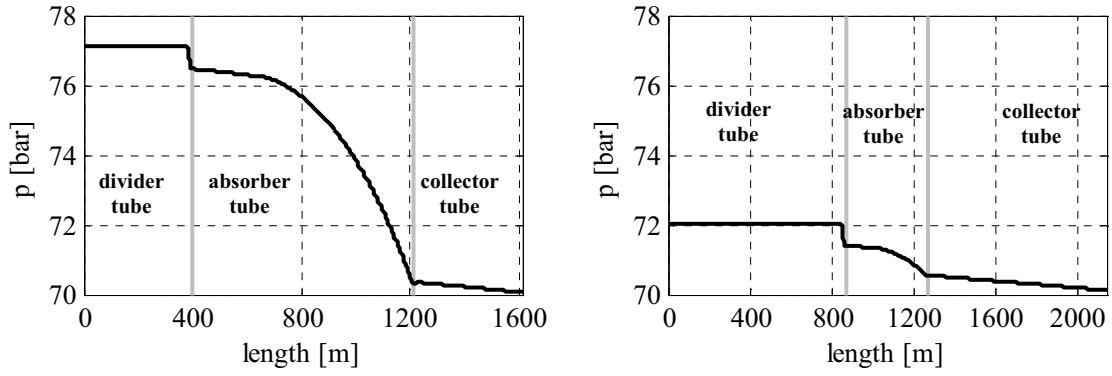

Figure 6: Variation of pressure from the feed water storage to the drum for layout 1 (left) and layout 2 (right)

Another effect is caused by the height difference of approximately 10 meters between the divider and the absorber tubes. This results in a static pressure drop right before the inlet of the evaporation field. The effect is negligible at the outlet of the evaporation field due to the significantly lower density of the two-phase fluid.

4.2 *Adapting the length of the divider and collector tubes*

According to the overall setup, the lengths of the divider tubes to the relevant solar collector modules are different. As shown in eq. 4, the pressure drop through the tubes is a linear function of the length of the tube. If the other parameters remain constant, the amount of pressure drop through the distant modules is much higher compared to those closer to the center of the evaporation field. Due to the fact that the overall system is closed, the resulting outlet pressure of all modules is the same. This also applies to the inlet pressure of each module. Therefore, the mass flow through the distant modules is reduced so that the pressure drop over all modules is equalized. Different mass flow results in different steam content at the outlet of modules as shown in figure 7 (left).

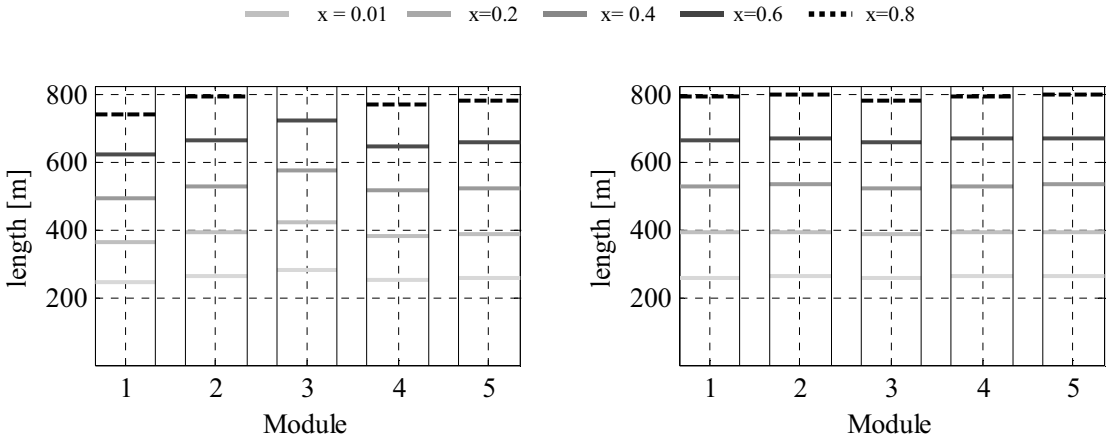

Figure 7: Variation of steam content in each solar collector module with equal (left) and adapted (right) tube diameters

It can also be seen that the steam content grows faster in the distant modules. Over the entire system the steam content varies in a range of 71% (center module) up to 87% (distant module). As a critical case superheating may occur in the distant modules, while the steam content in the center modules is close to design conditions. There are two possibilities to avoid this effect and to equalize the steam content, as well as other steam characteristics at the outlet of all modules. As the first opportunity, the mass flow in each module can be directly controlled. This method needs an active influence on the system. On the other hand, a passive approach adapts the diameter of the divider tubes, despite the fact that the friction pressure drop may be affected by the diameter of the tube as well. The necessary adaptions are shown in table 2.

Table 2: Diameters of divider and collector tubes

Number of module	**1**	**2**	**3**	**4**	**5**
Original diameter [m]	0.310	0.310	0.310	0.310	0.310
Adapted diameter [m]	0.290	0.255	0.190	0.270	0.260

Figure 7 (right) shows that the resulting mass flows and steam contents are almost equal. This is also valid for different load-cases. For the following simulations, these adaptions are used.

4.3 *Disturbances on the gained heat by absorber tubes*

Disturbances like clouds cause a sudden decrease in the DNI. Due to this, an imbalance between mass flow and heat could occur. To show the effects on the plant behavior, the nominal boundary conditions are changed to a partial load situation. The total mass flow is therefore reduced to 75% of the design mass flow, assuming that the amount of DNI is reduced to 75% by some clouds.

In a further simulation, the DNI is reduced to 50% assuming that the shading is getting bigger. In another simulation, the DNI is increased to 90%, assuming that the cloud is disappearing. These two cases are shown in figure 8 and compared to the partial-load simulation with 75% heat. For every simulation, the total mass flow remains constant at 75% of the design mass flow.

Regarding the steam content shown in figure 8 (right), the effect of the changed heat is clearly visible. If the DNI is increased, the steam content is rising, in the other case it is decreasing. But for every case, the starting point of the evaporation remains at the same position. The explanation for this behavior can be found regarding the temperature profiles in figure 8 (left). Due to the lower amount of steam in the case of reduced DNI, more water with saturation temperature is produced and circulated. The temperature of the mixture of circulated saturated water and pre-heated feed water is rising when the amount of saturated water rises ($T_{\text{saturation}}>T_{\text{feed water}}$). This results in a higher inlet temperature.

Regarding the pressure drop in figure 8 (middle), the big influence of the two-phase flow on the pressure drop can be seen. If the steam content increases, the amount of pressure drop increases.

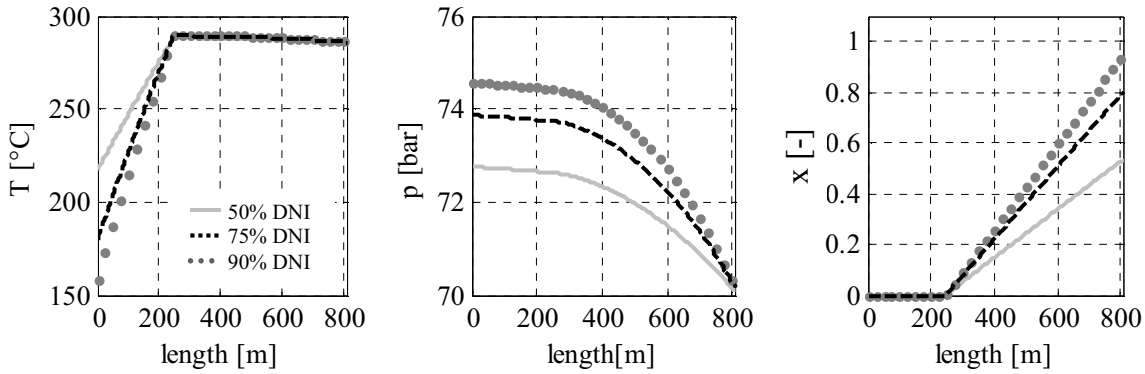

Figure 8: Variation of temperature, pressure and steam content along absorber tubes for different amounts of DNI

4.4 *Defocusing the reflector panels*

In power plant operation it is necessary to properly react to disturbances in the working conditions. Therefore, the behavior of the CSP plant is analyzed assuming a complete solar collector module is shadowed and bypassed from the entire network. In this simulation the mass flow remains on the design level. The resulting curves are shown in figure 9.

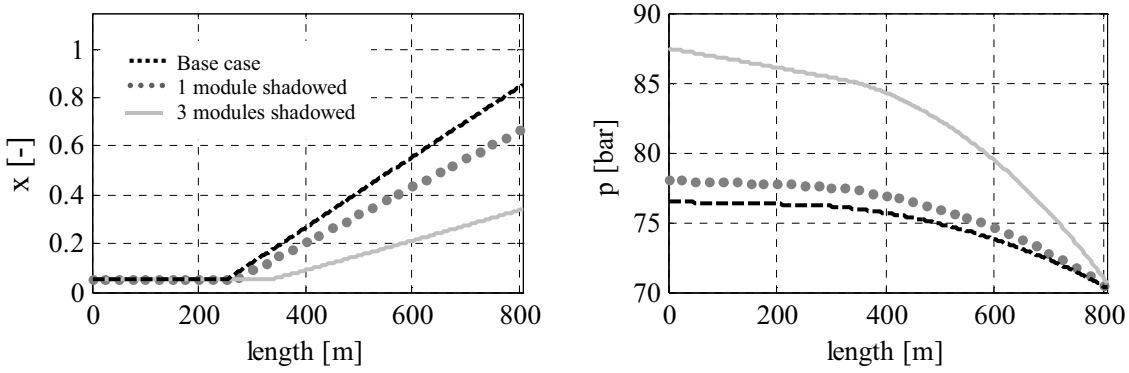

Figure 9: Variation of steam content and pressure for different solar collector modules shadowed

Due to the higher mass flow through the remaining modules, a higher pressure drop occurs through the entire evaporation field. If there is only one module bypassed, this pressure drop remains in a non-critical area. If the number of shadowed solar collector modules increases, the amount of the total pressure drop rises critically and provides undesired changes in the produced steam characteristics. Therefore, it is essential to adapt the mass flow inside the absorber tubes in order to the limit the changes to a tolerable level.

Another investigation concerns the control of several basic solar collector modules. The solar evaporation field is typically oversized during the design process, in order to produce more steam during the high consumption loads. At lower capacities, it is possible to set some reflector panels out of the focus and reduce the gained heat by the absorber tubes. In general, it is only possible to put a complete base collector out of the focus. Figure 10 shows the simulation results for defocused reflector panels at different positions along a single absorber tube in layout 2. It can be seen that the outlet steam content does not depend on the position of the defocused basic collector module. Nevertheless, it provides different behavior regarding the pressure. Because the pressure drop depends strongly on the local steam content, the pressure difference between two opposite heads of the absorber tube is bigger if the defocused panels are located at the end of the tube. So, from an operational point of view, the performance of the system improves when the defocused basic collector is positioned closer to the beginning of the absorber tube. This provides lower total pressure drop. However, concerning the automatic control of the system, it would be more appropriate to defocus the reflector panels closer to the outlet of the tubes. Doing so, the subsequent changes in the steam parameters can be observed and controlled faster.

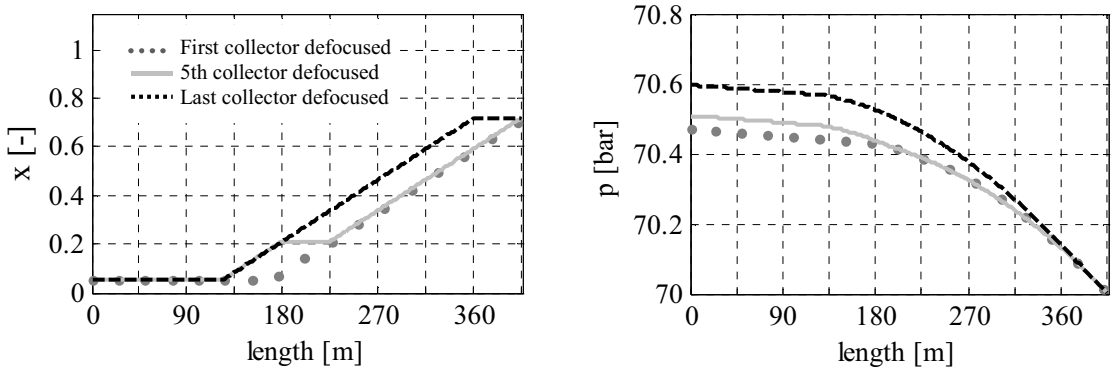

Figure 10: Variation of steam content and pressure for different defocused reflector panels along an absorber tube

4.5 *Further simulations regarding superheating*

In order to increase the efficiency of the solar power plant, an additional superheating solar field can be added after the evaporation field so that a higher steam temperature is achieved, and therefore, higher amount of energy can be produced. To analyze different possible superheating field setups, an EBSILON® Professional model, based on real power plant equipment data, is generated as shown in figure 11.

Using this model, several design possibilities of the water-steam-cycle are compared and two of them are explained as follows. First, the possibility to reheat the steam behind the high pressure steam turbine with either saturated or superheated steam is investigated. The second point of investigation concerns the condensate recirculation behind the steam drum.

The investigation of the reheating system shows that both types of steam (saturated and superheated) can be used very well as a heating medium. The mass flows of saturated and superheated steam are limited to the maximum, which still allows complete condensation of the steam. The amount of additional energy usable from the superheated steam is relatively small in comparison to the usable energy of the saturated steam. Therefore, only a small increase in the reheated steam temperature is achievable (approximately 10 K) when using superheated steam as superheating medium.

The evaporator field delivers saturated steam and partially saturated water to the steam drum, which is positioned between the evaporator- and the superheater field. This helps to avoid dry out at the end of the absorber tubes and supports a balanced operation of the evaporator. In the steam drum, the water is separated from the steam. The superheater field is then supplied with saturated steam from the steam drum. The saturated water of the steam drum then has to be recirculated.

The commonly used recirculation pump behind the steam drum often proves to be a challenge to be controlled in coordination with the feed water pump. In this model the feed water pump is divided into two

groups of pumps, and a collector was placed between the pumps. The pressure gradient between steam drum and collector allows feeding the saturated water from the steam drum into the steam collector without using an additional pump. Inside the steam collector, the saturated water is mixed with the feed water which avoids cavitation in the second feed water pump downwards the collector.

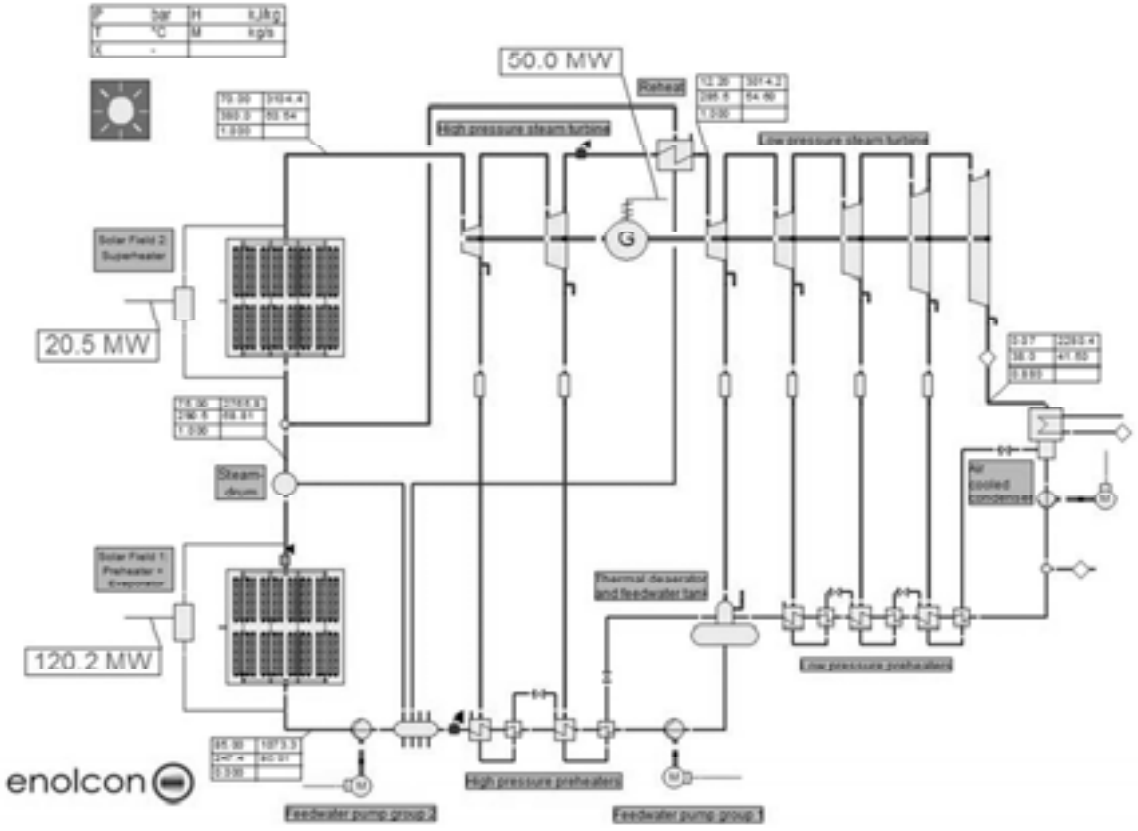

Figure 11: Model of a Linear Fresnel CSP Plant in EBSILON® Professional

5. Summary and outlook

A stationary 1-D CFD model of a Linear-Fresnel CSP was developed. Different simulations were done to get an impression of the general behavior of the plant. Detailed studies of a single heated pipe and the whole plant show that the pressure drop over the whole field is an important factor. The stationary model was developed out of an existing and validated model for fossil fuel fired plants. Different changes and adaptions were implemented to the model regarding the requirements of a CSP plant. The simulation results regarding disturbances prove the necessity of proper reactions to such disturbances in order to eliminate changes in the produced steam characteristics. For this goal, the mass flow of the feed water plays a substantial role. The simulation results show that it is also possible to react to some disturbances by defocusing the mirrors of the base collectors.

As an outlook for further works, the development of a control concept regarding the presented boundary and load conditions is essential. Therefore, it is necessary to implement a detailed dynamic model of the Linear-Fresnel CSP plant. With such a model different control approaches could be implemented and compared. Moreover, the simulation results with EBSILON show that an increase in the efficiency is possible by adding a superheating stage and optimizing the overall setup of the plant. In a next step this optimization setup must be applied with the CFD simulations to get a better understanding of the behavior of the superheating stage with a special emphasis on the critical points.

6. Acknowledgment

The presented work is part of an ongoing joined research and development project for improved automation and control concepts for Linear Fresnel power plants between the IFK University of Stuttgart and enolcon gmbh. The project is sponsored by the German Federal Ministry of Economics and Technology (BMWi) within the ZIM program (Central Innovation Program for small and medium sized business), project funding number KF 2530202DF0.

References

Eck, M., Hirsch, T., 2007. Dynamics and control of parabolic trough collector loops with direct steam generation, Solar Energy 81, 268-279

Facao, J., Oliveira, A., 2010. Simulation of a linear Fresnel solar collector concentrator, Journal of Low-Carbon Technologies

Friedel, L., 1978. Druckabfall bei der Strömung von Gas/Dampf-Flüssigkeits-Gemischen in Rohren, Chem.-Ing.-Tech. 50, 167-180

Novatec Biosol AG, 2009. The future. Today. PE1-Weltweit erstes Fresnel-Solarkraftwerk im kommerziellen Betrieb, Karlsruhe

SCHOTT Solar CSP GmbH, 2009. Schott PTR 70 Receiver, Mitterteich

Solarpraxis. http://www.renewables-made-in-germany.com/uploads/pics/Schema_Fresnel-Technol_opt.jpeg, Date: 28.07.11

Weidmann, M. 2009. Erstellung eines Referenzfalls zur Simulation von Naturumlaufdampferzeugern, Studienarbeit Nr. 2939, Institut für Feuerungs- und Kraftwerkstechnik (IFK), Universität Stuttgart